NEOPLASIA
www.neoplasia.com

Volume 11 Number 5 May 2009 pp. 426–435 426

In Vivo Antitumor and Antimetastatic Activity of Sunitinib in Preclinical Neuroblastoma Mouse Model[1]

Libo Zhang*,†, Kristen M. Smith†, Amy Lee Chong‡, Diana Stempak†,‡, Herman Yeger†,§, Paula Marrano†, Paul S. Thorner†, Meredith S. Irwin‡,§, David R. Kaplan‡,§ and Sylvain Baruchel*,‡,§

*New Agent and Innovative Therapy Program, The Hospital for Sick Children, Toronto, Canada; †Department of Paediatric Laboratory Medicine, The Hospital for Sick Children, Toronto, Canada; ‡Division of Hematology and Oncology, Department of Paediatrics, The Hospital for Sick Children, Toronto, Canada; §Institute of Medical Sciences and Department of Molecular Genetics, University of Toronto, Toronto, Canada

Abstract

Neuroblastoma (NB) is one of the most common pediatric solid tumors originating from the neural crest lineage. Despite intensive treatment protocols including megatherapy with hematopoietic stem cell transplantation, the prognosis of NB patients remains poor. More effective therapeutics are required. High vascularity has been described as a feature of aggressive, widely disseminated NB. Our previous work demonstrated the overexpression of vascular endothelial growth factor (VEGF) in NB, and we showed that an anti–VEGF receptor (VEGFR-2) antibody could induce sustained NB tumor suppression and regression. Sunitinib is a kinase inhibitor targeting platelet-derived growth factor receptors and VEGFRs and, therefore, a promising antiangiogenic agent. In this study, we investigated the antitumor activity of sunitinib and its synergistic cytotoxicity with conventional (cyclophosphamide) and novel (rapamycin) therapies. Both NB cell lines and tumor-initiating cells from patient tumor samples were used in our *in vitro* and *in vivo* models for these drug testing. We show that sunitinib inhibits tumor cell proliferation and phosphorylation of VEGFRs. It also inhibits tumor growth, angiogenesis, and metastasis in tumor xenograft models. Low-dose sunitinib (20 mg/kg) demonstrates synergistic cytotoxicity with an mTOR inhibitor, rapamycin, which is more effective than the traditional chemotherapeutic drug, cyclophosphamide. These preclinical studies provide the evidence of antitumor activity of sunitinib both in the early stage of tumor formation and in the progressive metastatic disease. These studies also provide the framework for clinical trial of sunitinib, alone and in combination with conventional and novel therapies to increase efficacy and improve patient outcome in NB.

Neoplasia (2009) 11, 426–435

Introduction

There has been considerable evidence *in vivo*, including clinical observations, that abnormal angiogenesis is correlated with active tumor growth, metastatic potential, and poorer patient prognosis in a variety of malignancies. Among the angiogenic growth factors, the vascular endothelial growth factors (VEGFs) and their corresponding receptor tyrosine kinases (RTKs; VEGFR-1 [fms-related tyrosine kinase 1 {Flt-1} 1], VEGFR-2 [Flk-1, kinase insert domain receptor {KDR}], and VEGFR-3 [Flt-4]) play an indispensable role in modulating angiogenesis and in the induction of vascular permeability and inflammation [1–4]. Antiangiogenic therapies based on the inhibition of

Address all correspondence to: Sylvain Baruchel, New Agent and Innovative Therapy Program, The Hospital for Sick Children, 555 University Ave, Toronto, Ontario, Canada M5G 1X8. E-mail: sylvain.baruchel@sickkids.ca

[1]This work was supported by Pfizer, Inc, James Birrell Neuroblastoma Research Fund, National Cancer Institute of Canada, Canadian Stem Cell Network, the Terry Fox Cancer Institute, and Solving Kids' Cancer.
Received 14 January 2009; Revised 19 February 2009; Accepted 22 February 2009

Copyright © 2009 Neoplasia Press, Inc. All rights reserved 1522-8002/09/$25.00
DOI 10.1593/neo.09166

VEGF/VEGFR signaling were reported to be powerful and well-tolerated therapy for solid tumors.

Neuroblastoma (NB) is the most common extracranial tumor of childhood accounting for 7.2% cancers in children younger than 15 years [5]. Despite intensive multimodality clinical trials, including the use of rescue autologous hematopoietic stem cell transplantation, survival remains poor at less than 30% in patients with metastatic disease [6]. Vascular endothelial growth factor (particularly its isoform, $VEGF_{165}$) and its receptors VEGFR-1/2 have been found to be upregulated in various NB cell lines and in advanced high stage (III/IV) NB [7,8]. Although VEGF primarily acts to promote angiogenesis, it may also function as a paracrine angiogenic factor and acts as an autocrine growth factor to promote NB cell growth directly [9]. In addition, VEGF, through its effects on vascular permeability, results in increased interstitial pressure, which inhibits the diffusion of chemotherapy agents into the tumor tissue.

Sunitinib (SU011248) is a novel small molecule multitarget inhibitor of RTKs, an important family of growth factor receptors. It has been shown in preclinical and clinical trials to have a direct antitumor effect in addition to targeting RTKs, specifically the platelet-derived growth factor receptor (PDGFR), VEGFR, KIT, Flt-3, and RET, against many different malignancies including acute myeloid leukemia, lung, colorectal, breast cancer, renal cell carcinoma, and thyroid carcinoma [10–15].

Rapamycin (RAP) is a potent inhibitor of phosphatidylinositol 3-kinase (PI3K)/Akt pathway by targeting mTOR (mammalian target of rapamycin). Possible additional mechanisms, through the reduction of VEGF levels and vascular AKT inhibitor with consecutive inhibition of angiogenesis, have been described as well. Its anticancer effect against different types of cancer has been demonstrated [27]. Conventional chemotherapeutics protocols use a multimodality approach often with high-dose chemotherapy, which is often associated with significant toxicities and treatment break to allow for hematopoietic recovery. Low-dose metronomic chemotherapy (LDM), the chronic administration of low doses of an antineoplastics agent, results in the inhibition of tumor growth by direct cytotoxicity and also by an antiangiogenic action targeting tumor vasculature [16]. The low therapeutic doses equate to minimal treatment breaks thereby not allowing for tumor regrowth and reducing drug resistance while minimizing acute/chronic chemotoxicities. In this study, we evaluated both NB cell lines and tumor-initiating cells (TICs) in *in vitro* studies and *in vivo* local and metastatic xenograph murine models to investigate the role of sunitinib in NB tumor growth, angiogenesis, and metastases. We hypothesized that combining sunitinib with other antiangiogenic therapy would suppress tumor growth and metastasis more durably than a single agent. Combination studies with rapamycin and LDM agents, cyclophosphamide, were expected to augment the individual antiangiogenic effect of each agent alone.

Materials and Methods

Materials

Sunitinib (SU011248), (*Z*)-*N*-[2-(diethylamino)ethyl]-5-[(5-fluoro-2-oxo-1,2-dihydro-3*H*-indol-3-ylidene)methyl]-2,4-dimethyl-1*H*-pyrrole-3-carboxamide (*S*)-2-hydroxysuccinate (Mr 398.48), was provided by Pfizer (Groton, CT). Antibodies were obtained from Santa Cruz Biotechnology (Santa Cruz, CA) and Cell Signaling Technology (Beverly, MA). The antiphosphotyrosine 4G10 antibody was obtained from Millipore (Billerica, MA).

Cell Lines

SK-N-BE(2) and SH-SY5Y cells were obtained from ATCC (Manassas, VA). LAN-5 cells were kindly provided by Dr. Robert Seeger (Children's Hospital Los Angeles), and NUB-7 cells were from Dr. Herman Yeger (The Hospital for Sick Children, Toronto, Ontario, Canada). Tumor-initiating cells (NB12, NB25, and NB88R2) were kindly donated by Dr. Kaplan's laboratory [16]. Neuroblastoma cell lines were cultured in α-minimum essential medium with 10% heat-inactivated fetal bovine serum at 37°C and harvested during exponential growth for use, storage, or further passage. Tumor-initiating cells were maintained in Dulbecco's modified Eagle's medium: F-12 (3:1, Invitrogen, Carlsbad, CA) with 2% B-27 supplement (Invitrogen), 40 ng/ml basic fibroblast growth factor (Collaborative, Boston, MA), 20 ng/ml epidermal growth factor (Collaborative), and 100 U/ml penicillin/streptomycin.

Nonobese Diabetic–Severe Combined Immunodeficiency Mice

Nonobese diabetic–severe combined immunodeficiency (NOD/SCID) mice (Jackson Laboratory, ME) were used for local and metastatic xenograft mouse models at 4 weeks of age. The mice were housed in an isolated sterile containment facility and fed *ad libitum* with water and food pellets. The Animal Care Committee at the Hospital for Sick Children approved the study. During the study, the mice were observed daily for possible adverse effects of medications, signs of ill health such as ruffled/thinning fur, abnormal behaviors, or local erosion from the tumor.

Cell Viability Assay

Cells were seeded into 24-well tissue culture plates at a density of 200,000 cells per well in culture medium and incubated for 24 hours at 37°C before starting drug treatment. Cells were exposed to increasing concentrations of sunitinib for 72 hours. The viability of proliferating cells in the control and treated media were measured with an Alamar Blue assay according to manufacturer's protocol (Trek Diagnostics Systems, Inc, Cleveland, OH). Briefly, Alamar Blue was diluted 1:10 in the cell culture media, and the fluorescent color change was monitored after 3 hours. Colorimetrical evaluation of cell proliferation was performed using a SPECTRAmax Gemini spectrophotometer with 540 nm as excitation wavelength and 590 nm as emission wavelength, and values were expressed as relative fluorescence units.

Sphere Formation Assay

Cells were seeded in triplicate in 96-well non–tissue culture treated plates at 3000 cells per well (2000 cells per well for NB12) in 50 μl of culture medium. Compounds were diluted to the indicated concentrations and immediately added to seeded cells in a volume of 50 μl, bringing the final volume to 100 μl. Wells were retreated with compound at the indicated concentrations 3 days after plating. Cultures were fixed with 4% paraformaldehyle (Electron Microscopy Sciences, Hatfield, PA) at day 7, and the number of spheres was determined manually. The percentage of control sphere number was calculated as follows: (mean sphere number for treated wells / mean sphere number of 0.05% DMSO-treated wells) × 100.

Xenograft Development

Two xenograft mouse models were used in this study. For the localized NB xenograft models, SK-N-BE(2) cells (10^6 cells/ml) or

NB12 cells (30,000) were injected into the subcutaneous groin fat pad of the NOD-SCID mice. Tumor size was measured weekly in two dimensions, and treatment started when tumor volume reached approximately 0.5 cm^3. For metastatic SK-N-BE(2) xenograft models, cells (10^6 cells/ml) were resuspended in 0.1 ml of sterile phosphate-buffered saline (PBS) and injected intravenously through the lateral tail vein of the NOD-SCID mice.

Drug Treatment

Sunitinib (Sutent; Pfizer) was prepared according to manufacturer's instructions and were stored as 100-μg/ml aliquots at −20°C. It was administered by daily gavage at incrementally increasing doses of 20, 30, and 40 mg/kg in a dextrose-water vehicle. Rapamycin was administered daily by intraperitoneal injection at a dose of 3 mg/kg. Cyclophosphamide was administered in the drinking water at a dosage of 20 mg/kg per day as previously described [17].

An initial dose-response study was performed using both SK-N-BE (2) and NB12 cells in localized xenograft mouse models. When the tumor volumes reached approximately 0.5 cm^3, the mice were randomized into four groups: control group and three groups assigned to receive escalating doses of sunitinib (20, 30, and 40 mg/kg). Sunitinib was administered by daily gavage, and the dextrose-water vehicle was used alone for the control group. Mice were killed after 14 days, and tumors were harvested and weighted. Two independent experiments were performed for each treatment with five to six animals per group. The optimal dose at which a response was demonstrated was identified and used in further experiments. A dose-response study was also performed using SK-N-BE(2) metastatic xenograft mouse models. Sunitinib was administered 2 weeks after tumor inoculation at the same dose as described for the localized model. Mice were killed after 14 days of drug treatment. Organs, including liver, lung, kidney, and femur, were harvested for histological diagnosis to determine the presence of metastases. Cardiac tissue was hematoxylin and eosin–stained and examined for evidence of cardiomyopathy.

Immunohistochemistry

A wedge section of each tumor was snap frozen in liquid nitrogen and analyzed for microvessel density by immunofluorescence using the endothelial cell marker CD34. After blocking with 4% BSA for 1 hour, slides were incubated with the primary antibody for CD34 (Ab8158-100, 1:50 dilution; Abcam, Cambridge, MA) overnight at 4°C followed by secondary fluorescein isothiocyanate AffiniPure donkey antirabbit immunoglobulin G (711-095-152, 1:200 dilution; Jackson ImmunoResearch Laboratories, West Grove, PA) for 1 hour at −4°C. Slides were analyzed for microvessel density with fluorescent microscopy.

Paraffin-embedded tumors were analyzed for microvessel density by immunostaining with the endothelial cell marker von Willebrand factor. Briefly, sections of paraffin-embedded tumors were incubated overnight with polyclonal rabbit antihuman von Willebrand factor antibody (no. A0082; DakoCytomation, Glostrup, Denmark) at 4°C. All slides were subsequently washed three times in PBS and incubated with a 1:100 dilution of biotin-conjugated donkey antirabbit immunoglobulin G (Jackson ImmunoResearch Laboratories) for 1 hour at room temperature. Slides were incubated with VECTASTAIN Elite ABC Kit (Vector Laboratories, Burlingame, CA) for 30 minutes at room temperature and then with DAB until desired staining was achieved, followed by counterstaining with hematoxylin. To quantify tumor angiogenesis, three high-power (×400) fields of the highest vascular density were digitally captured. Tumor angiogenesis is quantified and shown as a bar graph by the pixel values for positive von Willebrand factor staining using Image J software.

Enzyme-Linked Immunosorbent Assay

At time of sacrifice, blood was collected from SK-N-BE(2) metastatic model and plasma was analyzed for VEGF, VEGFR-1, and VEGFR-2 expression using quantikine ELISA kit from the R&D Systems (Minneapolis, MN) according to the manufacturer's instruction.

Vascular Endothelial Growth Factor Receptors Phosphorylation Assay

SK-N-BE(2) cells were grown for 48 hours to approximately 80% confluency before the experiment. Sunitinib was added in two dilutions (20 and 50 ng/ml) and incubated with cells for 1 hour at 37°C in culture medium without fetal bovine serum, followed by stimulation with $VEGF_{165}$ 50 ng/ml at 37°C for an additional 5 minutes. The cells were then lysed in lysis buffer (50 mM Tris-HCl, pH 7.4, 150 mM sodium chloride, 5 mM EDTA, 1 mM EGTA, 1% NP-40, 2 mM sodium *ortho*-vanadate, 1 mM phenylmethylsulfonyl fluoride, 5 μg/ml aprotinin, and 8 μg/ml leupeptin). Nuclei were removed by centrifugation for 10 minutes at 4°C. Protein concentrations of the lysates were determined using BSA as a standard. Immunoprecipitation was conducted using anti–Flt-1 and anti–Flk-1 antibodies. Proteins were resolved with SDS-PAGE and subjected to Western blot analysis. To detect phosphorylation, blots were probed with an antiphosphotyrosine monoclonal antibody, 4G10, and the same Western blot analysis was probed with anti–Flt-1 and anti–Flk-1 antibodies. All signals were detected using Super Signal West Pico Chemiluminescent Substrate (Pierce, Rockford, IL).

RNA Extraction

SK-N-BE(2) cells were cultured in fresh medium with or without 10 ng/ml of sunitinib for 3 hours. Total RNA was isolated and purified using ArrayGrade Total RNA Isolation Kit (SABiosciences, Frederick, MD) according to the manufacturer's instruction.

Microarray Analysis

Biotin-labeled complementary RNA was synthesized from 5 μg of total RNA using the TrueLabeling-AMP 2.0 Kit (SABiosciences) according to the manufacturer's instructions. The labeled complementary RNA samples were hybridized to the nylon membrane printed with 113 specified genes related to tumor angiogenesis. Data were analyzed using GEArray Expression Analysis Suite software. Changes in gene expression of more than two-fold were defined as significant.

Statistical Analysis

The data are presented as mean ± SE of the indicated number of independent experiments. Statistical analysis was performed by nonparametric analysis of variance of multiple comparisons using Fisher's least significant difference. $P < .05$ was considered to be significant.

Results

Effect of Sunitinib on NB Cell Lines

To study the cytotoxic effects of sunitinib, the NB cell lines, SK-N-BE(2), NUB-7, SH-SY5Y, and LAN-5, were exposed to increasing concentrations of sunitinib for 48 hours. As shown in Figure 1*A*,

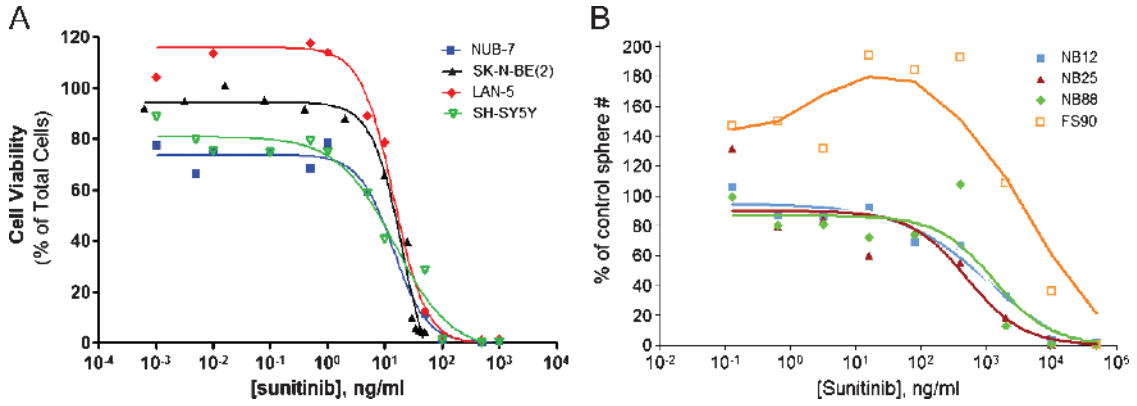

Figure 1. *In vitro* antitumor effect of sunitinib on NB cell line and TIC lines. (A) Dose-response plot of NB cell lines after sunitinib treatment. Neuroblastoma cell lines, SK-N-BE(2), NUB-7, SH-SY5Y, and LAN-5, were exposed to increasing concentrations of sunitinib for 72 hours and assayed with the AlamarBlue Cell Viability Assay. (B) A dose-response curve was generated by testing sunitinib against three TIC lines (NB12, NB25, and NB88R2) and normal skin-derived precursor cells (FS90). Sphere formation assay was used for *in vitro* testing, and spheres are counted after 7 days of treatment.

sunitinib significantly inhibited NB cell proliferation in a concentration-dependent manner. Plotting the log of the sunitinib concentrations, we determined that the IC_{50} of sunitinib is approximately between 10 and 20 ng/ml, which is within the clinically relevant human trough serum concentration (50-100 ng/ml).

Effect of Sunitinib on TICs from Primary NB

We next assessed the activity of sunitinib on TICs isolated from the bone marrow of unfavorable prognosis NB patients. These TICs have been reported to have characteristics of cancer stem cells and form metastatic NBs after orthotopic injection into immunodeficient

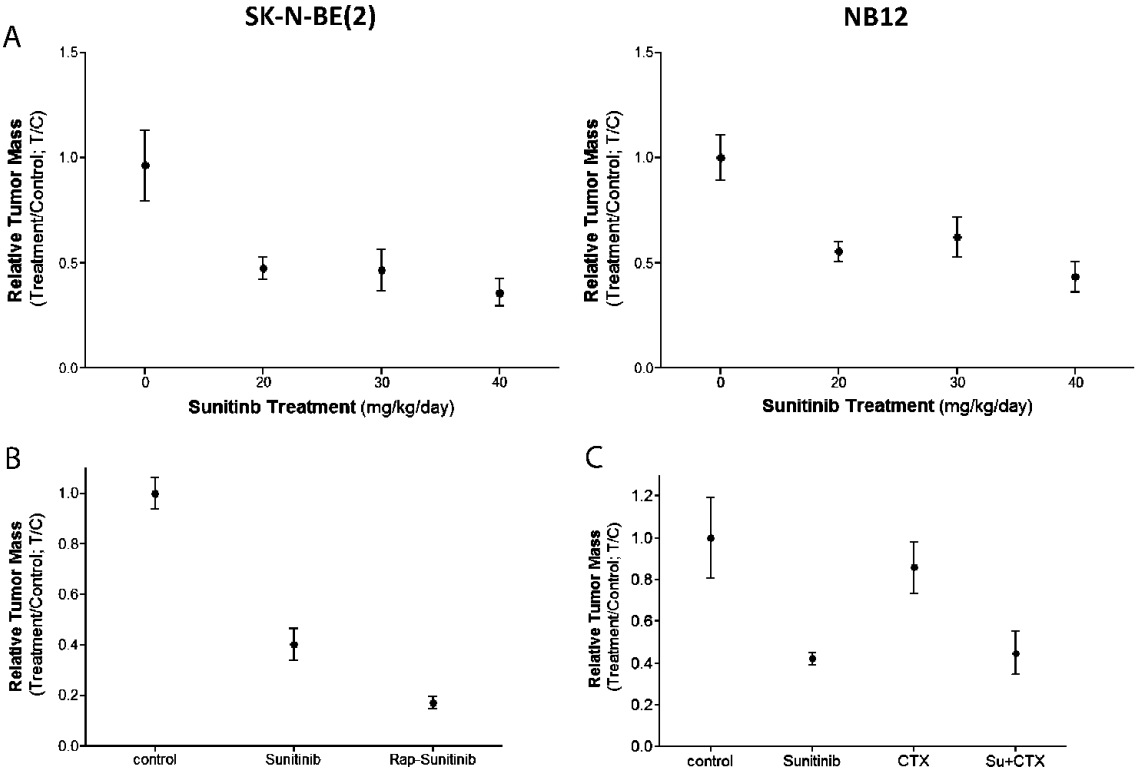

Figure 2. Effect of oral sunitinib on growth of established human NB in NOD/SCID mice. In localized NB xenograft model, 1×10^6 SK-N-BE(2) or 30,000 of NB12 cells were injected subcutaneously into the inguinal area of NOD-SCID mice. All treatment started when the tumor reached 0.5 cm in diameter. Two independent experiments were performed for each treatment with five to six animals per group. (A) Sunitinib was administered by gavage daily at three different doses (20, 30, or 40 mg/kg). Mice were killed after 14 days of treatment, and tumors were dissected and weighed. Drug activity was defined by tumor growth delay and optimal T/C (T/C – average treated tumor mass/average control tumor mass). (B, C) Antitumor activity of sunitinib, cyclophosphamide, rapamycin, and their combinations. Sunitinib was administered at 20 mg/kg, rapamycin (RAP) at 3 mg/kg daily intraperitoneally, and cyclophosphamide (CTX) orally through the drinking water at the approximate dosage of 20 mg/kg per day.

mice with as few as 10 cells. [18]. As shown in Figure 1*B*, three TIC lines from different patients (NB12, NB25, and NB88R2) responded to sunitinib treatment. The IC_{50} of sunitinib is approximately 10^3 ng/ml. We also assessed the effect of Sunitinib on nontransformed human pediatric neural crestlike stem cells, line FS90 (skin-derived precursors) [18]. The IC_{50} for cytotoxicity on FS90 was approximately 10 μg/ml.

Determination of Antitumor Effect of Sunitinib in NOD/SCID Mice

It has been shown by Fiebig [19] that xenograft models from fresh tumor explants can be predictive of clinical outcome. We therefore tested the ability of Sunitinib to affect tumor growth of SK-N-BE(2) cells and TICs (NB12) in a murine localized xenograft tumor model and in a metastatic model.

Localized xenograft tumors were established by the subcutaneous inoculation of tumor cells into NOD/SCID mice. Drug activity was defined by tumor growth delay and optimal T/C (T/C – average treated tumor mass/average control tumor mass). As shown in Figure 2*A*, treatment with 20 mg/kg of sunitinib showed significant reduction ($P < .05$) in primary tumor growth (%T/C: 49% for SK-N-BE(2) and 55% for NB12 tumor), whereas no significant difference was observed among doses 20, 30, and 40 mg/kg. Because the 20-mg/kg dose seemed to have an effect that was similar to that of either 30 or 40 mg/kg, 20 mg/kg was determined to be the optimal dose to be used in the combination drug treatments.

We also compared the effect of sunitinib in combination treatment with cyclophosphamide or rapamycin. Sunitinib was administered at 20 mg/kg by gavage, in combination with rapamycin 3 mg/kg daily intraperitoneally and cyclophosphamide orally through the drinking water at the approximate dosage of 20 mg/kg per day. In the localized tumor model, sunitinib, as a single agent, demonstrated superior activity than cyclophosphamide did. Combined therapy was more effective in achieving an overall reduction in tumor volume when sunitinib was used in conjunction with rapamycin ($P < .05$; Figure 2*B*).

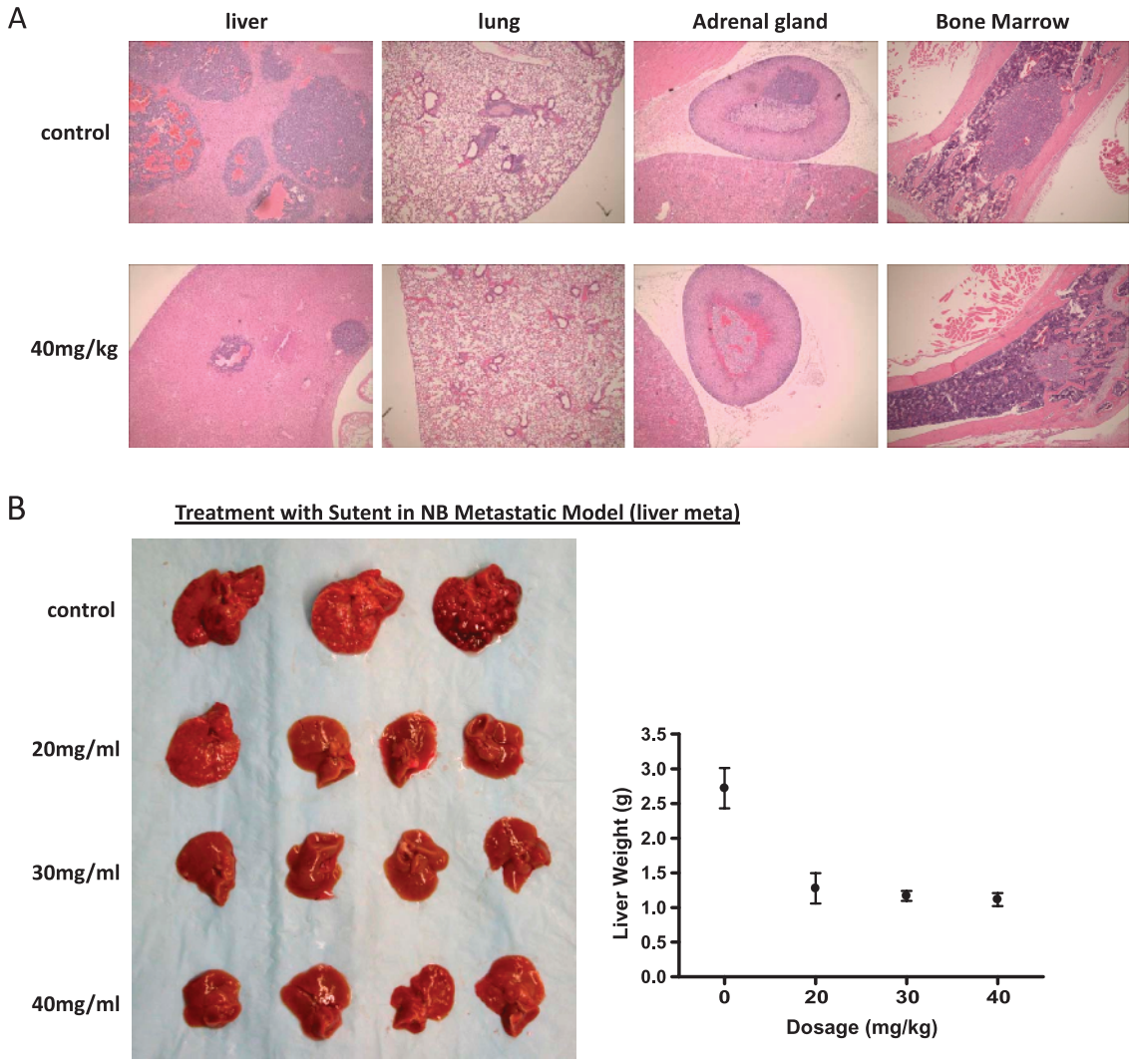

Figure 3. The effect of sunitinib in NB metastasis formation. In our metastatic model, 1×10^6 SK-N-BE(2) cells were injected intravenously through the lateral tail vein. Sunitinib treatment started 2 weeks after intravenous inoculation. Mice were killed after 14 days treatment for the evaluation of metastases by both optical image and histology. (A) Only mice in control group showed signs of distress and developed extensive liver metastasis and ascites. In the sunitinib treatment groups, only few scattered metastatic nodules were observed. Histology slides showed significant deduction of number and size of metastatic sites in liver, lung, adrenal gland, and bone marrow after treatment with sunitinib. (B) A significant difference in liver weight between control and all treatment groups ($P < .01$).

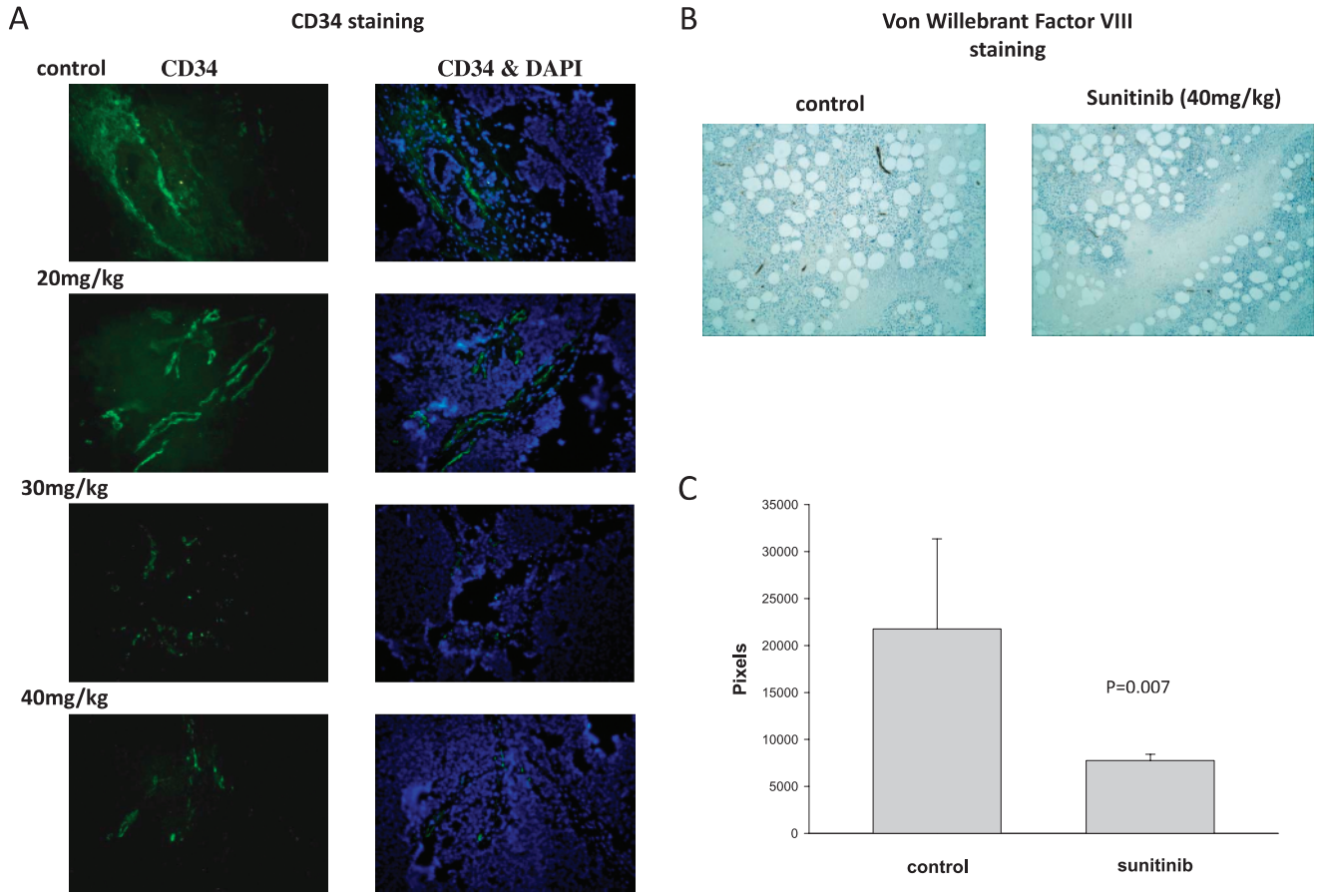

Figure 4. The effect of sunitinib on NB tumor angiogenesis. Tumor samples from the above xenograft model were analyzed for microvessel density. (A) Microvessels were identified by the endothelial cell maker, CD34, with immunofluorescence staining, whereas tumor tissue was identified by 4′, 6-diamidino-2-phenylindole staining. (B) Microvessels were also identified by immunohistochemical staining for von Willebrand factor by immunohistochemistry. Positive immunohistochemical (brown) staining indicates the presence of endothelial cells and microvessel structure in tumor tissues. (C) To quantitate the antiangiogenic effect of sunitinib, three fields with tumor angiogenesis from each von Willebrand factor–stained tumor section were digitally captured. Tumor angiogenesis is quantified and shown as a bar graph by the pixel values for positive von Willebrand factor staining using Image J software.

Although sunitinib and cyclophosphamide administered together significantly reduced tumor volume, there is no significant change when compared with sunitinib monotherapy (Figure 2*C*).

Efficacy of Sunitinib on NB Tumor Metastasis

For the metastatic model, mice were injected intravaneously with 10^6 SK-N-BE(2) cells, and the cells were allowed to implant for 7 days. After 7 days, the animals were treated either with PBS or with different doses of sunitinib (20, 30, 40 mg/kg) for 14 days (Materials and Methods), at which point all animals were euthanized, and necroscopy was performed. The peritoneal cavity of each animal was photographed, histology was performed, and the occurrence of tumors was noted in the following organs: liver, lung, kidney, adrenal gland, and bone marrow. Only mice in the control group showed signs of distress and developed extensive liver metastasis and ascites. Gross examination and histology of different organs showed a dramatic decrease in the numbers and size of metastatic sites formed in the treated animals compared with the control group (Figure 3*A*). We also observed a significant difference in liver weight between control and all treatment groups ($P < .01$; Figure 3*B*). Thus, sunitinib shows significant efficacy for treatment of NB metastasis.

Efficacy of Sunitinib on NB Tumor Angiogenesis

Tumor samples from the above xenograft models were analyzed immunohistochemically using the endothelial markers von Willebrand factor and CD34 to determine the extent of angiogenesis. As shown in Figure 4*A*, with increasing dose of sunitinib from 20 to 40 mg/kg, a lower density of microvessels appeared in the tumor tissues, indicating a dose-dependent inhibition.

To quantitate the antiangiogenic effect of sunitinib, three hot spots from each von Willebrand factor–stained tumor were digitally captured. The software, Image J, assigns pixel values for positive von Willebrand factor staining (Figure 4*B*), and the average of all the pixels in all the tumors found in each treatment group is shown as a bar graph (Figure 4*C*). Sunitinib (40 mg/kg) inhibited tumor angiogenesis by 36% ($P = .007$).

Sunitinib Inhibits VEGF-Triggered Phosphorylation of VEGFRs

Because sunitinib is effective as an antiangiogenic agent, we performed further studies to investigate whether this treatment could also affect the *in vitro* and *in vivo* production of VEGF as well as modulate the expression and phosphorylation of its receptors in plasma by ELISA

at the end of treatment. No appreciable changes in VEGF and VEGFRs plasma levels were observed after sunitinib treatment (Figure 5*A*).

We also investigated whether sunitinib could abrogate VEGF-induced VEGFRs tyrosine phosphorylation in NB cells. As shown in Figure 5*B*, sunitinib inhibited VEGF-induced VEGFR-2 (Flk-1) tyrosine phosphorylation at 20 ng/ml as well as VEGFR-1 (Flt-1) phosphorylation at 50 ng/ml. Taken together, these data indicated that sunitinib blocks VEGF-triggered pathways by inhibiting VEGFRs phosphorylation, likely contributing to its antitumor effects in NB cells.

Regulation of Angiogenesis-Related Genes by Sunitinib

Although we know that sunitinib inhibits RTKs, specifically the PDGFR, VEGFR, KIT, FLT-3, and RET, little is known about

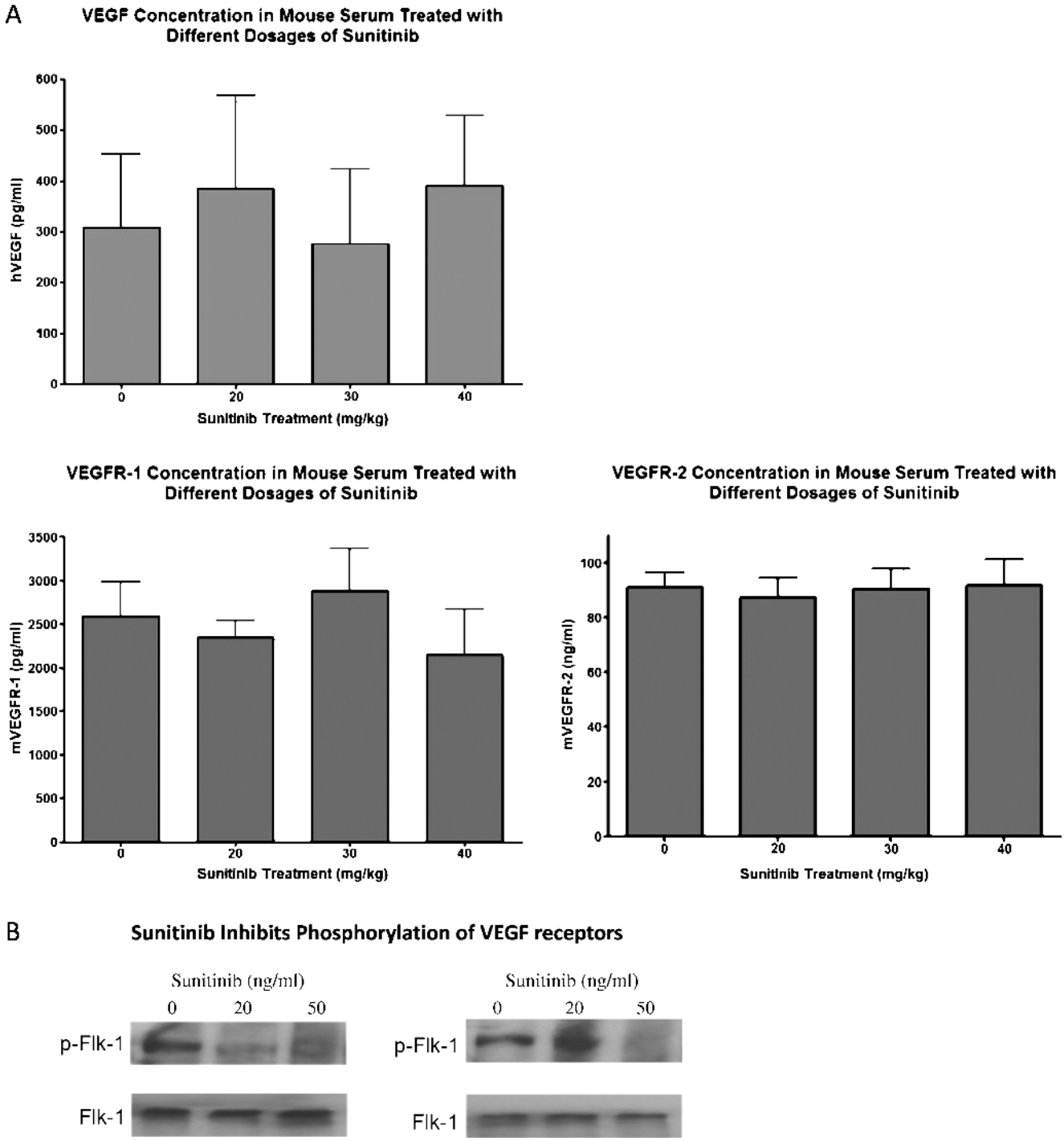

Figure 5. Inhibition of VEGF-induced phosphorylation of VEGFRs by sunitinib. (A) The plasma concentrations of VEGF and VEGFRs (VEGFR-1 and VEGFR-2) were determined by ELISA at the end of sunitinib treatment. (B) SK-N-BE(2) cells were incubated with 20 or 50 ng/ml of sunitinib for 1 hour and then stimulated with 50 ng/ml VEGF for 5 minutes at 37°C. Vascular endothelial growth factor receptors were immunoprecipitated from cell lysates. Western blot analysis was performed on immunoprecipitates with an antiphosphotyrosine antibody (upper panel) and polyclonal anti-VEGFR antibodies (lower panel).

complex interactions between these factors and their cooperative effects in promoting tumor angiogenesis and metastasis. To address the genetic mechanisms by sunitinib, altering the expression of other genes related to tumor metastasis, we performed cDNA microarray analyses. We screened the NB cell line, SK-N-BE(2), with 113 genes that have been reported to be involved in modulating tumor angiogenesis and compared this gene profile to the same cell line after treatment with sunitinib. Changes in gene expression of more than two-fold were defined as significant. In 34 genes extracted from the microarray data, as shown in Table 1, only 1 gene, angiogenin (ANG), showed marginal increase (2.04-fold) after sunitinib treatment, and other 8 genes downregulated after treatment. Among these downregulated genes are transcription factors (*HIF1A*), growth factors and receptors (*EFNA2*, *PDGFB*, and *VEGFC* and *EDG1*, respectively), and other angiogenic factors (*AGGF1* and *PTEN*).

Discussion

High vascularity has been described as a feature of aggressive, widely disseminated NB. Expression of VEGF is nearly ubiquitous in NB primary tumors and has been demonstrated in all NB cell lines tested to date, and high-circulating VEGF and basic fibroblast growth factor levels were correlated with high-risk NBs. Increased primary tumor VEGF expression, particularly $VEGF_{165}$, correlates significantly with advanced (stages III and IV) disease [7,8]. In our previous publications, we demonstrated that VEGFR-2 and, to a lesser degree, VEGFR-1 are expressed within NB cell lines as well as primary NBs, and VEGF/Flt-1 pathway is critical in promoting NB growth under hypoxic conditions [20]. Sunitinib is a kinase inhibitor targeting multiple RTKs, including PDGFRs and VEGFRs. Preclinical and clinical studies using sunitinib showed tumor regression and prolonged survival in mammary adenocarcinoma, melanoma, and leukemia [21–24]. Here, we investigated the effect of sunitinib in NB preclinical models and compared with LDM therapy on NB tumor growth, angiogenesis, and metastasis. Our data demonstrated that sunitinib provided significant anticancer activity against NB, and this effect was greater than LDM therapy alone.

Rapamycin is a potent inhibitor of PI3K/Akt pathway and it inhibits the activity of a protein called mTOR, a serine-threonine kinase member of the cellular PI3K pathway. The PI3K/Akt/mTOR pathway plays a central role in cell survival and proliferation. It is also involved in the production of proangiogenic factors (e.g., VEGF) and in endothelial cell proliferation [25,26]. Inhibition of several steps of this pathway has been shown to confer favorable antitumor activity in a variety of cancer types [27]. In preclinical studies, inhibiting mTOR with RAD001 diminished the expression of VEGF in tumor-derived cell lines and inhibited angiogenesis *in vivo* [28]. In this study, rapamycin proved to be effective when used in combination with sunitinib. Therefore, combining sunitinib and rapamycin could potentially be a more effective therapy in the NB clinic. Work in our laboratory is being done to further elucidate the mechanism of rapamycin action and whether there is an additive antiangiogeneic effect.

Table 1. Angiogenesis Genes Regulated by Sunitinib Treatment in Microarray Analysis.

Symbol	Description	Level Change After Treatment
ANG	Angiogenin, ribonuclease, RNase A family, 5	204.62%
FGFR3	Fibroblast growth factor receptor 3 (achondroplasia, thanatophoric dwarfism)	199.17%
EFNA1	Ephrin-A1	190.55%
NRP1	Neuropilin 1	174.21%
NUDT6	Nudix (nucleoside diphosphate linked moiety X)-type motif 6	154.34%
EFNB2	Ephrin-B2	152.99%
ANGPT2	Angiopoietin 2	149.26%
LAMA5	Laminin, alpha 5	147.18%
ECGF1	Endothelial cell growth factor 1 (platelet-derived)	146.69%
NOTCH4	Notch homolog 4 (*Drosophila*)	132.08%
VEGFB	Vascular endothelial growth factor B	121.87%
MDK	Midkine (neurite growth-promoting factor 2)	121.45%
CXCL5	Chemokine (C-X-C motif) ligand 5	121.43%
PTN	Pleiotrophin (heparin binding growth factor 8, neurite growth-promoting factor 1)	119.37%
KDR	Kinase insert domain receptor (a type III RTK)	119.16%
TIMP1	TIMP metallopeptidase inhibitor 1	116.96%
ENG	Endoglin (Osler-Rendu-Weber syndrome 1)	107.43%
PGF	Placental growth factor, VEGF–related protein	101.50%
TIMP3	TIMP metallopeptidase inhibitor 3 (Sorsby fundus dystrophy, pseudoinflammatory)	99.95%
CXCL9	Chemokine (C-X-C motif) ligand 9	99.02%
AKT1	V-akt murine thymoma viral oncogene homolog 1	96.64%
SERPINF1	Serpin peptidase inhibitor, clade F (alpha-2 antiplasmin), member 1	91.24%
IL1B	Interleukin 1, beta	72.30%
AS1R2	Artificial sequence 1 related 2 (80% identity) (48/60)	59.59%
EFNA3	Ephrin-A3	56.87%
MMP2	Matrix metallopeptidase 2 (gelatinase A, 72-kDa gelatinase, 72-kDa type IV collagenase)	55.20%
PTEN	Phosphatase and tensin homolog (mutated in multiple advanced cancers 1)	49.77%
HIF1A	Hypoxia-inducible factor 1, alpha subunit (basic helix-loop-helix transcription factor)	48.53%
AGGF1	Angiogenic factor with G patch and FHA domains 1	45.38%
VEGFC	Vascular endothelial growth factor C	42.36%
EDG1	Endothelial differentiation, sphingolipid G-protein–coupled receptor, 1	41.46%
PDGFB	Platelet-derived growth factor beta polypeptide (simian sarcoma viral (v-*sis*) oncogene homolog)	38.44%
EFNA2	Ephrin-A2	37.27%
TIMP3	Tissue inhibitors of metalloproteinase 3 (Sorsby fundus dystrophy, pseudoinflammatory)	32.80%

The intensity of shaded area represents the different expression levels of genes. The darkest shade (>200%) represents a significant increase, whereas the lightest shade (<50%) represents a significant decrease of gene expression.

According to the cancer stem cell hypothesis, cancer stem cells are a minority of mutated stem cells or progenitors that have self-renewal properties and also give rise to the heterogeneous mixture of cells that make up the bulk of tumors [29]. Broad-spectrum chemotherapy may eliminate the tumor mass, but cancer stem cells seem more resistant than the rest of the tumor to cancer drugs and radiation [30]. Hence, treatments targeting tumor stem cells would be required. In this study, we isolated TICs from fresh samples of NB patients and used them in our *in vitro* and *in vivo* models for drug testing. These TICs have been shown to have tumor stem cell features in our published studies, and they are capable of generating localized tumors by inoculating as few as 50 spheres (approximately 3000 cells) [18]. Although the IC_{50} of sunitinib for TICs is much higher than that for NB cell lines, our *in vivo* results show that even at a lower dose (20 mg/kg), sunitinib has a similar antitumor effect between TICs and NB cell line. Combining the evidence of VEGF/VEGFR pathway on angiogenesis, our data suggest that the antitumor effect of sunitinib is more dependent on regulating tumor microenvironment and angiogenesis.

The concept of an "angiogenic switch" in stimulatory and inhibitory growth factors is important as angiogenesis is a key factor in the evolution of solid tumors, as in the presence of an inadequate blood supply they cannot exceed a critical mass size of 1 to 2 mm and are maintained in a steady state balance between cell proliferation and apoptosis [31]. The first antiangiogenesis drug approved by the Food and Drug Administration to treat cancer was bevacizumab (Avastin) in 2004. It is now used along with chemotherapy to treat some types of cancer [32–34]. Since then, several other drugs with antiangiogenic properties have been approved, including sorafenib [35] and sunitinib [36,37]. Despite current therapy-intensive multimodality protocols, the outcome of patients with aggressive/unfavorable histological finding, NB tumor remains poor. Using the NB cell line, SK-N-BE(2) and NB TICs, NB12, we demonstrated the therapeutic potential of a novel antiangiogenic agent, sunitinib, a multi-RTK inhibitor that proved to be able to block phosphorylation of the VEGFRs.

In human dose-finding studies, an oral dose of 50 mg/dose has been associated with tumor response in adult patients and a manageable toxicity profile [38]. Recently, congestive cardiac failure, reduction of left ventricular ejection fraction and hypertension have been described in adults treated with repeating cycles of sunitinib in phase 1/2 trials [39,40]. To lower the risk of drug adverse effects, we used a lower dose (20 mg/kg) of sunitinib combined with rapamycin. Compared with high-dose monotherapy (40 mg/kg), more significant antitumor effects were observed in combined treatment with low-dose sunitinib (20 mg/kg) and rapamycin. Also, histological studies of heart tissues did not show any evidence of cardiotoxicity (data not shown).

Although we know that sunitinib inhibits RTKs, specifically the PDGFR, VEGFR, KIT, Flt-3, and RET, little is known about the complex interactions between these factors and their cooperative effects in promoting tumor angiogenesis and metastasis. Our additional finding demonstrated that sunitinib not only regulates tumor angiogenesis through inhibiting tyrosine kinase receptors but also interacts with other tumor angiogenic factors, which may be an alternative mechanism of action of sunitinib. By blocking multiple angiogenic signaling pathways and their interactive loops, a better therapeutic effect could be achieved.

Acknowledgments

The authors thank Christine Mormont and Stephen Fields for their helpful comments. The authors thank Robert Seeger for the NB cell line, LAN-5. The authors greatly appreciate the support of NB patients and their families for the donation of samples. Thanks are also extended to Meredith S. Irwin for her coordinating in obtaining patient samples.

References

[1] Martiny-Baron G and Marme D (1995). VEGF-mediated tumour angiogenesis: a new target for cancer therapy. *Curr Opin Biotechnol* **6**, 675–680.

[2] McColl BK, Stacker SA, and Achen MG (2004). Molecular regulation of the VEGF family—inducers of angiogenesis and lymphangiogenesis. *APMIS* **112**, 463–480.

[3] Shibuya M and Claesson-Welsh L (2006). Signal transduction by VEGF receptors in regulation of angiogenesis and lymphangiogenesis. *Exp Cell Res* **312**, 549–560.

[4] Pradeep CR, Sunila ES, and Kuttan G (2005). Expression of vascular endothelial growth factor (VEGF) and VEGF receptors in tumor angiogenesis and malignancies. *Integr Cancer Ther* **4**, 315–321.

[5] SEER. Surveillance, Epidemiology, and End Results (SEER) Program Web site. Available at: http:www.seer.cancer.gov. Accessed 2003.

[6] Matthay KK and Cheung NKV (2005). Treatment of neuroblastoma—high risk neuroblastoma. In NKV Cheung and S Cohn (Eds.), *Neuroblastoma.* Heidelberg, Germany: Springer-Verlag Berlin, pp. 138–149.

[7] Meister B, Grünebach F, Bautz W, Brugger F, Fink M, Kanz L, and Möhle M (1999). Expression of vascular endothelial growth factor (VEGF) and its receptors in human neuroblastoma. *Eur J Cancer* **35**, 445–449.

[8] Eggert A, Ikegaki N, Kwiatkowski J, Zhao H, Brodeur GM, and Himelstein BP (2000). High-level expression of angiogenic factors is associated with advanced tumor stage in human neuroblastomas. *Clin Cancer Res* **6**, 1900–1908.

[9] Langer I, Vertongen P, Perret J, Fontaine J, Atassi G, and Robberecht P (2000). Expression of vascular endothelial growth factor (VEGF) and VEGF receptors in human neuroblastomas. *Med Pediatr Oncol* **34**, 386–393.

[10] O'Farrell AM, Abrams TJ, and Yuen HA (2003). SU11248 is a novel FLT3 tyrosine kinase inhibitor with potent activity *in vitro* and *in vivo*. *Blood* **2003**, 3597–3605.

[11] Abrams TJ, Lee LB, and Murray LJ (2003). SU11248 inhibits KIT and platelet-derived growth factor receptor in preclinical models of human small cell lung cancer. *Mol Cancer Ther* **2**, 471–478.

[12] Abrams TJ, Murray LJ, and Pesenti E (2003). Preclinical evaluation of the tyrosine kinase inhibitor SU11248 as a single agent and in combination with "standard of care" therapeutic agents for the treatment of breast cancer. *Mol Cancer Ther* **2**, 1011–1021.

[13] Burstein HJ, Elias AD, and Rugo HS (2008). Phase II study of sunitinib malate, an oral multitargeted tyrosine kinase inhibitor, in patients with metastatic breast cancer previously treated with an anthracycline and a taxane. *J Clin Oncol* **26**, 1810–1816.

[14] van der Veldt AMA, Meijerink MR, and van den Eertwegh AJM (2008). Sunitinib for treatment of advanced renal cell cancer: primary tumor response. *Clin Cancer Res* **14**, 2431–2436.

[15] Mendel DB, Laird AD, and Xin X (2003). *In vivo* antitumor activity of SU11248, a novel tyrosine kinase inhibitor targeting vascular endothelial growth factor and platelet-derived growth factor receptors. *Clin Cancer Res* **9**, 327–337.

[16] Klement G, Baruchel S, Rak J, Man S, Clark K, Hicklin DJ, Bohlen P, and Kerbel RS (2000). Continuous low-dose therapy with vinblastine and VEGF receptor-2 antibody induces sustained tumor regression without overt toxicity. *J Clin Invest* **105**, R15–R24.

[17] Emmenegger U, Shaked Y, Man S, Bocci G, Spasojevic I, Francia G, Kouri A, Coke R, Cruz-Munoz W, Ludeman SM, et al. (2007). Pharmacodynamic and pharmacokinetic study of chronic low-dose metronomic cyclophosphamide therapy in mice. *Mol Cancer Ther* **6**, 2280–2289.

[18] Hansford LM, McKee AE, Zhang L, George RE, Gerstle JT, Thorner PS, Smith KM, Look AT, Yeger H, Miller FD, et al. (2007). Neuroblastoma cells isolated from bone marrow metastases contain a naturally enriched tumor-initiating cell. *Cancer Res* **67**, 11234–11243.

[19] Fiebig H-H and Burger AM (1999). Relevance of Tumor Models for Anticancer Drug Development. *Contributions to Oncology* **54**, 462.

[20] Das B, Yeger H, Tsuchida R, Torkin R, Gee MF, Thorner PS, Shibuya M, Malkin D, and Baruchel S (2005). A hypoxia-driven vascular endothelial growth factor/Flt1 autocrine loop interacts with hypoxia-inducible factor-1alpha through mitogen-activated protein kinase/extracellular signal-regulated kinase 1/2 pathway in neuroblastoma. *Cancer Res* **65**, 7267–7275.

[21] Burstein HJ, Elias AD, Rugo HS, Cobleigh MA, Wolff AC, Eisenberg PD, Lehman M, Adams BJ, Bello CL, DePrimo SE, et al. (2008). Phase II study of sunitinib malate, an oral multitargeted tyrosine kinase inhibitor, in patients with metastatic breast cancer previously treated with an anthracycline and a taxane. *J Clin Oncol* **26**, 1810–1816.

[22] Cabebe E and Wakelee H (2006). Sunitinib: a newly approved small-molecule inhibitor of angiogenesis. *Drugs Today (Barc)* **42**, 387–398.

[23] Peterson AC, Swiger S, Stadler WM, Medved M, Karczmar G, and Gajewski TF (2004). Phase II study of the Flk-1 tyrosine kinase inhibitor SU5416 in advanced melanoma. *Clin Cancer Res* **10**, 4048–4054.

[24] Nishioka C, Ikezoe T, Yang J, Takeshita A, Taniguchi A, Komatsu N, Togitani K, Koeffler HP, and Yokoyama A (2008). Blockade of MEK/ERK signaling enhances sunitinib-induced growth inhibition and apoptosis of leukemia cells possessing activating mutations of the *FLT3* gene. *Leuk Res* **32**, 865–872.

[25] Kurmasheva RT, Harwood FC, and Houghton PJ (2007). Differential regulation of vascular endothelial growth factor by Akt and mammalian target of rapamycin inhibitors in cell lines derived from childhood solid tumors. *Mol Cancer Ther* **6**, 1620–1628.

[26] Li W and Sumpio BE (2005). Strain-induced vascular endothelial cell proliferation requires PI3K-dependent mTOR-4E-BP1 signal pathway. *Am J Physiol Heart Circ Physiol* **288**, H1591–H1597.

[27] Morgensztern D and McLeod HL (2005). PI3K/Akt/mTOR pathway as a target for cancer therapy. *Anticancer Drugs* **16**, 797–803.

[28] Huynh H, Chow KP, Soo KC, Toh HC, Choo SP, Foo KF, Poon D, Ngo VC, and Tran E (2008). RAD001 (everolimus) inhibits tumor growth in xenograft models of human hepatocellular carcinoma, *J Cell Mol Med*. 2008 May 10. [Epub ahead of print].

[29] Jordan CT (2004). Cancer stem cell biology: from leukemia to solid tumors. *Curr Opin Cell Biol* **16**, 708–712.

[30] Donnenberg VS and Donnenberg AD (2005). Multiple drug resistance in cancer revisited: the cancer stem cell hypothesis. *J Clin Pharmacol* **45**, 872–877.

[31] Bergers G and Benjamin LE (2003). Tumorigenesis and the angiogenic switch. *Nat Rev Cancer* **3**, 401–410.

[32] (2006). FDA approves Avastin in combination with chemotherapy for first-line treatment of most common type of lung cancer. *Cancer Biol Ther* **5**, 1425–1428.

[33] Emmanouilides C, Pegram M, Robinson R, Hecht R, Kabbinavar F, and Isacoff W (2004). Anti-VEGF antibody bevacizumab (Avastin) with 5FU/LV as third line treatment for colorectal cancer. *Tech Coloproctol* **8** (Suppl 1), s50–s52.

[34] Ferrara N, Hillan KJ, and Novotny W (2005). Bevacizumab (Avastin), a humanized anti-VEGF monoclonal antibody for cancer therapy. *Biochem Biophys Res Commun* **333**, 328–335.

[35] Lang L (2008). FDA approves sorafenib for patients with inoperable liver cancer. *Gastroenterology* **134**, 379.

[36] van der Veldt AA, Meijerink MR, van den Eertwegh AJ, Bex A, de Gast G, Haanen JB, and Boven E (2008). Sunitinib for treatment of advanced renal cell cancer: primary tumor response. *Clin Cancer Res* **14**, 2431–2436.

[37] Le Tourneau C, Raymond E, and Faivre S (2007). Sunitinib: a novel tyrosine kinase inhibitor. A brief review of its therapeutic potential in the treatment of renal carcinoma and gastrointestinal stromal tumors (GIST). *Ther Clin Risk Manag* **3**, 341–348.

[38] Faivre S, Delbaldo C, and Vera K (2006). Safety, pharmacokinetic, and antitumor activity of SU11248, a novel oral multitarget tyrosine kinase inhibitor, in patients with cancer. *J Clin Oncol* **24**, 25–35.

[39] Chu TF, Rupnick MA, and Kerkela R (2007). Sunitinib-related cardiotoxicity: an interdisciplinary issue. *Lancet* **370**, 2011–2019.

[40] Khakoo AY, Kassiotis CM, and Tannir N (2008). Heart failure associated with sunitinib malate. *Cancer* **112**, 2500–2508.